

Mitigating the Impact of Blockages in Millimeter-Wave Vehicular Networks Through Vehicular Relays

CAGLAR TUNC^{ID} (Graduate Student Member, IEEE), AND SHIVENDRA S. PANWAR^{ID} (Fellow, IEEE)

Department of Electrical and Computer Engineering, New York University Tandon School of Engineering, Brooklyn, NY 11201, USA

CORRESPONDING AUTHOR: C. TUNC (e-mail: ct1909@nyu.edu)

This work was supported in part by NYU Wireless, an Ernst Weber Fellowship and in part by the NY State Center for Advanced Technology in Telecommunications (CATT).

ABSTRACT With the high data rates and ultra-low latency it provides, millimeter-wave (mmWave) communications will be a key enabler for future vehicular networks. However, due to high penetration losses and high mobility, mmWave links experience frequent blockages. We present an analytical framework to evaluate the performance of vehicular relaying, where vehicles on a highway exchange data with the network, either over direct vehicle-to-infrastructure (V2I) links with roadside units or a combination of a vehicle-to-vehicle (V2V) sidelink and a V2I link. Both V2V and V2I line-of-sight links can be blocked by other vehicles. We establish continuous-time Markov chain models of the blockage events that V2I links and vehicular relays experience, and use their steady-state solution to obtain analytical expressions for the blockage probability, average blockage duration and the SINR distribution. We demonstrate through numerical examples that relays are helpful, especially when the traffic density is high, since they can provide intermittent but more frequent connection opportunities and reduce the blockage duration. We show that relays that are far from a vehicle only have a marginal benefit since they are blocked with higher probability, compared to the closer relays. The proposed analytical framework enables fast and accurate assessment of a given deployment scenario, which will benefit researchers exploring mmWave-enabled vehicular networks.

INDEX TERMS Latency, Markov analysis, millimeter wave (mmWave) communications, relay nodes, vehicle-to-everything (V2X) networks.

I. INTRODUCTION

WITH the increased deployment of connected vehicles, future vehicular networks will need to support use cases such as cooperative maneuvering, situation/event awareness, and video streaming, that can have high data rate (~ 0.1 -1 Gbps) and extremely low latency (~ 1 -10 ms) requirements [1]. These use cases aim to provide high safety, improved driving experience and, more importantly, high levels of autonomy, with reliable connectivity to the network. Considering the potential number of vehicles that are connected to the network, and the amount of traffic each of them exchanges, this requires a tremendous amount of bandwidth

and network capacity. Fifth generation (5G) networks will be a key driver for such use cases, since the main goal for the 5G systems is to satisfy stringent network requirements with high reliability and availability [2]. Employing millimeter-wave (mmWave) frequencies, 5G networks are envisioned to enable these services and use cases with different levels of data rate, latency and reliability requirements, such as enhanced mobile broadband (eMBB), massive machine-type communications (mMTC), ultra-reliable communications, and vehicle-to-everything (V2X) communications.

Although mmWave has the potential to provide the data rate and latency requirements for such use cases, achieving the network requirements with high reliability and availability is the main challenge at these frequencies. Due to high penetration loss at higher frequencies, mmWave radiowaves

The review of this article was arranged by Associate Editor Claudia Campolo.

experience frequent blockages and outages, which is an even bigger challenge to tackle in high mobility scenarios, such as vehicular networks [3]. Therefore, a well-considered approach is required to design and deploy mmWave wireless networks in order to address the aforementioned coverage challenges. There are several studies in the literature that consider mmWave communications for vehicular networks, including [4]–[12]. Most of these papers use mmWave channel models and tools from stochastic geometry to analyze the coverage probability, based on line-of-sight (LOS) and non-line-of-sight (NLOS) channel models and the resulting statistical signal-to-interference-noise-ratio (SINR) [4]–[7]. However, as we show in our initial work [8], the latency performance is a greater challenge for mmWave communications in vehicular networks. In terms of latency, there are relatively fewer related studies in the literature. The authors in [9] use an LOS/NLOS channel model, where the goal is to minimize an age of information metric with optimal resource allocation policies. In [12], the authors propose using backup NLOS links when LOS links are blocked to reduce a latency violation probability. In the literature, there are other studies that model the evolution of LOS and NLOS through simulations [10] and measurements [11]. However, as discussed in [10] and [11], the existence and robustness of NLOS links in a vehicular network depend on several factors, including the type/speed of the vehicles, receiver and transmitter antenna heights, the distance between antennas, locations and types of buildings/surroundings. Moreover, using mmWave frequencies for vehicular networks is more likely to provide benefits in the presence of LOS paths from the transmitter to the receiver [13]. Measurements show that blockages caused by large vehicles on a highway can attenuate the received signal power by more than 20 dB [14]. From a higher-layer perspective, small-scale fluctuations in the SINR when mmWave links are blocked cause challenges in higher layers, such as the transport layer, which jeopardizes the end-to-end performance [15]. Therefore, in order to accurately characterize the limitations of mmWave-enabled vehicular communications, we focus our analysis on LOS links.

In this study, we focus on a highway scenario where communicating vehicles (CVs) exchange data over mmWave vehicle-to-infrastructure (V2I) links with the roadside units (RSUs), which are deployed along one side of the highway and connected to the network with high speed wired or wireless backhaul. The LOS V2I links from CVs to RSUs can be obstructed by other vehicles. Such blockages can degrade the SINR by about 20 dB [16], [17]. As a widely used link model in the literature for mmWaves, we assume that LOS link blockages result in excessive degradation in SINR, and hence, loss of connectivity [12], [18]. Therefore, when all V2I links are blocked, a CV cannot establish a direct link to an RSU. On the other hand, if a CV can establish an LOS vehicle-to-vehicle (V2V) link with another CV, which has a direct V2I link to an RSU, then this V2V link can be used as a *sidelink* to reach the network. V2V sidelinks in a V2X ecosystem can provide data relaying opportunities to improve

coverage [19]. 3GPP Release 18 discusses several vehicular relay use cases to improve coverage and quality-of-service of mobile users from applicability, requirement, and security perspectives, which can be adapted to V2V sidelinks and V2V relaying for future standardization efforts [20]. For a more detailed discussion on different use cases and open research problems, such as security and inter-vendor operability, the reader is referred to [21].

We consider one-hop and two-hop connections for the communicating vehicles, which means that a CV either communicates with an RSU over a direct V2I link, or through a vehicular relay. As discussed in [22] for wireless local area networks (WLANs), increasing the number of hops in a traffic relaying network results in several challenges for the relay nodes. A two-hop connection between a vehicle and the infrastructure through a single vehicular relay is shown to improve the connectivity performance of the vehicle significantly [23]. On the other hand, further increasing the number of hops in the relay network results in diminishing performance improvement. For instance, considering a vehicular network with sidelinks, a relay CV has to use most of its allocated bandwidth/capacity for the relaying purposes, which introduces additional delays to its own transmissions. For a two-hop connection the delay can be minimized by optimizing the scheduling decisions as in [24]; however, the complexity of the delay control problem grows exponentially with the number of hops due to the exponentially growing number of connections. Moreover, the radio access network (RAN) and RSUs have to coordinate all the relayed traffic, which grows exponentially with the number of vehicles and the number of hops allowed to relay the traffic. All vehicles connected through sidelinks also need to coordinate and synchronize, in order to allocate resources and decode messages [19]. For a high-mobility scenario that is prone to frequent link blockages, such as the highway environment we consider, maintaining synchronization and coordination across vehicles becomes increasingly challenging as the number of vehicular hops increases. Therefore, in order to keep the complexity of traffic forwarding low, and other practicality issues, we only consider traffic relaying through a single V2V sidelink.

In our previous work [25], we analyzed LOS V2I links and obtained the blockage probability and the average blockage duration, for arbitrary vehicle classes with any given distribution for the vehicle dimensions. In this paper, we extend our analysis in [25] such that V2V sidelinks can be used in order to relay the traffic from a given CV. Our main goal is to provide an analytical framework that will enable fast and accurate analysis of a vehicular relay network, without the need to run long and extensive simulation. We focus on the performance evaluation in terms of three main metrics, namely the blockage probability, average blockage duration, and SINR distribution. To the best of our knowledge, the framework we propose in this paper is the first to provide analytical expressions for the blockage duration in a vehicular relay network. Moreover, we derive the distribution of the

SINR that a CV experiences, which is computed by taking into account the probabilities of having V2I and relay connections. Finally, we also examine the distribution of blockage duration obtained from the simulations and discuss how it is affected by the CV probability and vehicle speeds. We summarize the main findings of this paper as follows.

- Increasing the LOS range for a fixed number of RSUs to help the CV find more relays results in only a marginal benefit, since the blockage probability of a V2V sidelink increases with the distance between the CV and the candidate relay.
- As the traffic density increases, the blockage probability goes up due to more frequent blockages; but interestingly, the probability of finding a relay also increases, which provide short duration connections that help reduce the average blockage duration.
- The speeds of the vehicles affect the duration of V2V and V2I link blockages, and hence the overall blockage duration.
- Since the average SINR of direct V2I links are higher than that of a connection through a relay, the SINR of a CV decreases as V2I blockage probability increases.
- Having more CVs, which translates to more candidate relays, on the highway reduces the duration of blockages, and hence the blockage probability.
- Increasing the RSU density reduces the blockage probability and the average blockage duration. Moreover, deploying taller RSUs mainly eliminates short blockages while the remaining long blockages cause a larger average blockage duration. These findings are consistent with our observations in [25] for a V2I network.

The main contributions of this paper can be summarized as follows.

- We propose a continuous-time Markov chain model of blockages that occur in a vehicular relay network, where a mmWave-enabled vehicle communicates with the network over vehicular relays.
- The steady-state solution of the proposed model along with that of the Markov chain model for V2I connections is used to derive analytical expressions for the blockage probability, average blockage duration, and the SINR distribution.
- We investigate the impact of several highway and deployment-related parameters, such as the height and density of RSUs, speed and density of vehicles, on four useful metrics: the blockage probability, average blockage duration, distribution of blockage duration and SINR distribution.

The paper is organized as follows. We present the related work in Section II. In Section III, we describe different components of the system model, including the considered highway scenario, channel and communication models for the V2V sidelinks and V2I links, the blocking vehicle placement process and V2V link blockage evolution. We analyze the coverage performance and derive analytical expressions for

the blockage probability, the average blockage duration and the SINR distribution in Section IV. We validate the accuracy of the proposed analytical model, and demonstrate how different highway and deployment parameters affect the coverage performance in terms of the blockage probability, average blockage duration, SINR distribution and the distribution of blockage duration in Section V. In Section VI, we discuss the implications of our findings and conclude the paper.

II. RELATED WORK

In this section, we summarize the literature in three main related categories. First, we present the studies on the coverage performance of mmWave base stations (BSs) and RSUs, and then the ones considering mmWave V2V links. Finally, we discuss the studies on the latency performance of mmWave networks.

A. MMWAVE BS/RSU COVERAGE

There have been many studies analyzing the blockage of mmWave links and the resulting coverage performance in a vehicular network, in the context of BSs [4]–[7], [26]–[28] and RSUs [29]–[31]. Blockage of the LOS links due to large vehicles in the adjacent lane of a designated vehicle is investigated in [4], and the performance is analyzed in terms of coverage probability, throughput and link path gain. For the same metrics, the authors analyze an urban street-level setting in [26]. A similar blockage model is considered in [5] for a highway scenario where the vehicles in adjacent lanes block an LOS connection. A stochastic geometry-based analysis is derived to obtain LOS coverage probability and the distribution of coverage rate. Another paper that considers a highway scenario is [6], where the objective is to analyze the connectivity and find the beam coverage probability. A Markov chain formulation of blockages due to random blockers is established in [7]. In [27], the authors propose a deep learning-aided beam alignment mechanism to improve the performance of the mmWave system in terms of spectral efficiency and received signal strength. Kong *et al.* [29] outline the main characteristics of mmWave vehicular systems and provide a discussion on how to address mmWave design challenges, including deployment, beamforming and frequent handovers. In [30], for an urban environment, LTE and mmWave deployments are compared in terms of the average data rate and the outage probability. In [31], the goal is to analyze the optimal beamwidth and the beam alignment strategy to improve the data rate.

B. MMWAVE V2V MODEL AND COVERAGE

Since V2V communication at mmWave frequencies is proposed as a potential technology to improve data rates in vehicular networks, there have been several studies that report measurement results of mmWave V2V networks. The authors in [11] conduct measurements of mmWave V2V links between transmitter and receiver antennas, mounted

on mobile vehicles. Based on the measurements, a statistical model of the path loss is derived. This model shows that the links blocked by vehicles can experience an additional signal attenuation of 10-25 dB, depending on the distance between transmitter and receiver vehicles, and the number of vehicles blocking the LOS path simultaneously. This outcome is not surprising, especially considering that, even at sub-6 GHz frequencies, which are less prone to penetration loss and blockages, LOS and NLOS links with a single blocker show quite different path loss characteristics [32]. V2V link measurements at 73 GHz reported in [14] show that even a single blocker can result in an additional signal attenuation of over 20 dB. These results underscore the need to have an LOS link to ensure reliable communication, especially in a highway scenario where there are relatively fewer reflectors and scatterers, compared to an urban environment.

In a vehicular network with mmWave connections between vehicles and RSUs, using vehicular relays and V2V links to improve the coverage has been investigated in several studies, including [19], [33]–[36]. The analysis in [19] demonstrates that V2V sidelinks can be a promising technology to improve coverage and block-error-rate (BLER) performance of a V2X network. Optimal relay selection policies to minimize multi-hop relaying while satisfying average SINR requirements are investigated in [33]. In [34], it is shown that the coverage probability of V2I links can be improved with the help of vehicular relays operating at mmWaves. In the presence of blockage, the study in [35] proposes a connectivity control mechanism for mmWave vehicular relays to enhance the coverage of RSUs. Finally, the authors in [36] propose using a position-based mmWave beam alignment strategy for highway scenarios, rather than the standard beam-sweeping procedure, to improve the throughput performance.

C. MMWAVE LATENCY PERFORMANCE

All of the studies discussed above examine the coverage performance in terms of throughput, coverage probability, or an equivalent metric, considering LOS link blockages and/or NLOS links. However, there are relatively fewer papers focusing on the time an LOS link remains blocked, and the resulting delay performance of mmWave communications for vehicular networks, which, as we show in this paper, is the main performance limitation. In [28], for urban and rural environments, latency, average and 5th and 10th percentile throughputs measured at the User Datagram Protocol (UDP) layer are obtained through ns-3 simulations. In [37], autonomous vehicles connected to mmWave RSUs are considered and the main goal is to optimize the system performance by jointly considering latency and reliability. For different protocol layers and use types, such as eMBB, mMTC, and ultra-reliable low-latency communication (URLLC), latency and jitter values are investigated in [38], which does not consider any blockages. The authors in [9] and [39] use a so-called age of information (AoI) metric to quantify the latency for an URLLC system, considering a V2V setting. The goal of both papers is to avoid large AoI

metrics, which is an indicator of increased latency, where the optimal user grouping and power allocation policies are sought in [9] and [39], respectively.

III. SYSTEM MODEL

In this section, we describe the modeling of vehicles on a highway segment, and the LOS communication models of V2I and V2V links.

A. HIGHWAY MODEL

We consider a highway scenario with N_L lanes, each having a width of W_L , three types of vehicles, namely standard vehicle (SV), CV and blocking vehicle (BV). CVs and SVs have similar length and height statistics (such as passenger cars). The height of CVs and SVs is fixed and denoted by h_C , whereas their length is exponentially distributed with mean $1/\mu_C$. Both SVs and CVs move with a constant speed of V_C . On the other hand, BVs move with a constant speed of V_B , and belong to a vehicle class which is larger and higher in general (such as trucks/buses). We denote the fixed height of a BV by h_B , and the length of a BV is exponentially distributed with mean $1/\mu_B$. Note that, as we show in our previous work [25], the analysis presented in this paper works for more general height and length distributions, such as Gaussian. However, for tractability of the analysis, we assume fixed vehicle heights and exponentially distributed vehicle lengths in this paper. Without loss of generality, we assume throughout this paper that $h_B > h_C$ and $1/\mu_B > 1/\mu_C$, indicating that BVs have larger dimensions compared to CVs and SVs on average. Moreover, unlike SVs and BVs, CVs are equipped with antennas and communication systems that operate in mmWave frequencies. A random vehicle in a given lane belongs to one of the three types of vehicles, CV, SV and BV, with probabilities p_C , p_S and p_B , respectively. Our goal is to analyze the coverage of CVs, whose goal is to exchange data with the network through the RSUs that are located along the roadside of the right-most lane.¹ In order to model the traffic intensity, we use an exponential distribution with mean $E[d]$ for the distance between the rear bumper of a vehicle and the front bumper of the following vehicle, which is also in agreement with the model in [40]. The average inter-vehicle distance $E[d]$ depends on the traffic density of the considered scenario. A large average inter-vehicle distance is an indicator of a low traffic density, and vice versa.

B. CHANNEL MODEL

In order to tackle high path loss and signal attenuation at mmWave frequencies, beamforming is used to generate extremely narrow and directional beams. In this paper, we consider such narrow and directional beams, and ignore the interference from other V2V/V2I links. Physical blockage of these beams by other vehicles in a vehicular environment, such as trucks, results in a signal attenuation by

¹We assume, without loss of generality, right-hand traffic in this paper.

around 20 dB [14]. In a highway scenario with high-speed transmitters/receivers, rapid signal fluctuations present additional challenges to maintain reliable NLOS links, such as fast beam tracking and recovery [41]. Moreover, reflective surfaces, such as buildings and other structures needed to establish NLOS links may not be present in rural highway environments [42]. Therefore, in this paper, we focus on an on-off blockage model, where the links that are blocked by vehicles are assumed to be in outage. We assume both V2V and V2I LOS links experience Rayleigh fading with mean $1/\mu$, i.e., $h \sim \exp(\mu)$, where h denotes the small scale fading component of the link. We consider a block-fading channel model where the channel coefficient remains constant over a frequency-time block. We use standard power attenuation to model the path loss of an LOS link as $d^{-\alpha}$ [4], where d is the Euclidean distance between the transmitter and receiver, and α is the LOS path loss exponent. Hence, the received SINR for the LOS links is described as

$$\frac{P_T h d^{-\alpha}}{N_0}, \quad (1)$$

where P_T is the transmit power and N_0 is the noise power.

C. COMMUNICATION MODEL FOR V2I LINKS

Lanes are assumed to be indexed from 1 to N_L , starting from the rightmost (slowest) lane. Without loss of generality, we focus our analysis on a CV that drives along the center of lane i for $i = 2, \dots, N_L$. We consider the BVs in lanes $j = 1, \dots, i-1$ driving along the centers of their lanes as the potential blockers of the LOS V2I links. In order to reach the network, a CV, say CV_1 , in lane i for $i = 2, \dots, N_L$, first attempts to establish an LOS V2I link to an RSU. If such link exists, then CV_1 can use this link to exchange data with the network, and therefore is said to be in coverage. On the other hand, these V2I links can be blocked by BVs in lanes $j = 1, \dots, i-1$. In particular, if a BV intersects the LOS path between a CV and an RSU, that particular RSU is said to be blocked and is not reachable by the CV through a direct V2I link. If all V2I links are blocked, in order to reach the network, CV_1 can establish a V2V link to another CV, say CV_2 , which is in coverage by at least one RSU through a V2I link. In this case, CV_2 serves as a vehicular relay for CV_1 and forwards the traffic between the network and CV_1 .

Given the channel model described in Section III-B, the received SINR at a given Euclidean distance determines whether a packet can be successfully received or not. For analytical tractability of the blockage model, we assume that there exists a fixed communication range for the CVs, denoted by R , such that any data sent over an LOS V2V or V2I link that has a Euclidean distance less than R can be successfully decoded at the receiver. In other words, as illustrated in Figure 1, we assume that a CV can reliably communicate with an RSU over a V2I link or with a CV over a V2V link if the length of the link is less than R , and not blocked by any BV. We denote the length of the

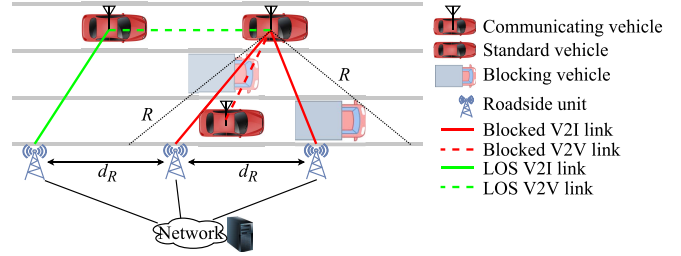


FIGURE 1. Example network with $N_L = 3$, $N_R = 2$.

road segment for which all RSUs have a point-to-point link distance shorter than R to the CV by R_C , which is the horizontal distance between the intersection points of two dotted lines with the roadside in Figure 1. We refer to R_C as the *coverage range*. We assume that the inter-RSU distance, denoted by d_R , is chosen such that $N_R = R_C/d_R$ is an integer. Therefore, N_R denotes the number of RSUs that lie within the LOS coverage range of the CV. Note that without this assumption, the communicating vehicle can be in the range of either $\lfloor N_R \rfloor$ or $\lceil N_R \rceil$ RSUs. Using the proportions of time that the vehicle is served by $\lfloor N_R \rfloor$ and $\lceil N_R \rceil$ RSUs, one can relax the assumption that N_R is an integer and generalize the analysis presented in this paper. However, we keep this assumption for analytical tractability.

We assume that RSUs are deployed at a fixed height, denoted by h_R . We are interested in scenarios where the maximum value of h_R is limited by the highway regulations, cost, and the availability of existing structures on which RSUs can be deployed, and therefore blockages due to BVs cannot be completely eliminated by increasing the RSU heights indefinitely.

Depending on CV, BV and RSU antenna heights, lanes $1, \dots, i-1$ can potentially block LOS links between a CV in lane i and RSUs, for $i = 2, \dots, N_L$. A BV in lane $j = 1, \dots, i-1$ will block the CV if its height is larger than the critical height of lane j , denoted by $h_B^{(i,j)}$, which is given by:

$$h_B^{(i,j)} \triangleq h_C + (h_R - h_C) \frac{i-j}{i-\frac{1}{2}}. \quad (2)$$

We compute the LOS coverage range of a communicating vehicle in lane i as follows:

$$R_C = 2\sqrt{R^2 - |h_R - h_C|^2 - \left[\left(i - \frac{1}{2}\right)W_L\right]^2}. \quad (3)$$

Note that increasing h_R results in fewer lanes potentially blocking a communicating vehicle, but also a smaller coverage area R_C . We illustrate the geometry of equations (2) and (3) for $i = 3$ in Figure 2.

D. COMMUNICATION MODEL FOR V2V LINKS

Similar to the V2I link model, two CVs can establish a V2V link if the LOS path is not blocked by a BV, and the distance between the CV antennas is less than R . A potential V2V link between two CVs in lane i and j for $i, j = 1, \dots, N_L$

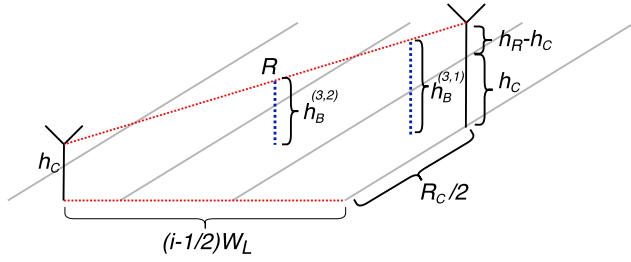


FIGURE 2. Illustration of equations (2), (3) for $i = 3$.

can be blocked by one or more BVs in the lanes in between, as well as lanes i and j , as illustrated in Figure 1.

E. MODEL OF BLOCKING VEHICLE PLACEMENT PROCESS

For a given probability distribution for each vehicle type in a lane, we use a two-state continuous time Markov chain, as proposed in [25] and illustrated in Figure 3, to model the BV placement. This is a simplified two-state model of the underlying vehicle type distribution that characterizes whether a vehicle can block an LOS V2I link or not. For the scenario we consider, since SVs and CVs have the same height, only BVs can block the LOS V2I links. The rates of this model are derived using the length distribution of BVs and the average distance between two BVs, which we also refer to as the inter-BV distance. These rates, which have a unit of $1/\text{m}$, will be combined with vehicle speeds and used to compute the transition rates of the Markov chain formulation. According to this model, for a CV in lane i , inter-BV distances and BV lengths in lane j are exponentially distributed with means $1/\lambda_B^{(i,j)}$ and $1/\mu_B$, respectively, for $j = 1, \dots, i-1$. $\lambda_B^{(i,j)}$ refers to the BV arrival rate and is computed in the following proposition.

Proposition 1: For a CV in lane i , BV arrival rate in lane j , for $j = 1, \dots, i-1$, is given by:

$$\lambda_B^{(i,j)} = \begin{cases} \left(\frac{1-p_B}{p_B} (1/\mu_C + E[d]) + E[d] \right)^{-1}, & h_B > h_B^{(i,j)} \\ 0, & h_B \leq h_B^{(i,j)}. \end{cases} \quad (4)$$

Proof: If $h_B \leq h_B^{(i,j)}$, no vehicle in lane j can block the LOS link, thus $\lambda_B^{(i,j)} = 0$. For the case $h_B > h_B^{(i,j)}$, let $\bar{D}_B^{(i,j)} = 1/\lambda_B^{(i,j)}$ denote the average inter-BV distance. Also, let N_C denote the number of vehicles of type CV or SV in between two BVs. Given N_C , we write the average inter-BV distance, denoted by $\bar{D}_{B|N_C}^{(i,j)}$, as follows:

$$\bar{D}_{B|N_C}^{(i,j)} = N_C(1/\mu_C + E[d]) + E[d], \quad (5)$$

since there are N_C vehicles, each of which has a mean length of $1/\mu_C$, and $N_C + 1$ inter-vehicle distances with a mean of $E[d]$ each. Since each vehicle in a lane belongs to types SV, CV and BV with probabilities p_S , p_C , and p_B , respectively, N_C follows a geometric distribution with a success probability of p_B . Therefore, if we take the expectation of (5) over

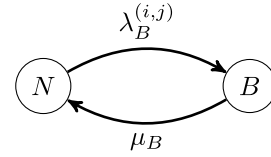


FIGURE 3. BV placement process for V2I link analysis in lane j for a CV in lane i , where N and B denote no-BV and BV states, respectively.

N_C , we have:

$$\bar{D}_B^{(i,j)} = E[N_C](1/\mu_C + E[d]) + E[d] \quad (6)$$

$$= \frac{1-p_B}{p_B} (1/\mu_C + E[d]) + E[d], \quad (7)$$

which completes the proof. ■

F. MODEL OF VEHICLE-TO-VEHICLE SIDELINK BLOCKAGES

In order to model the blockages that V2V LOS links experience, we use a two-state continuous time Markov chain, given in Figure 4. The given system models the state of V2V sidelinks between a designated CV in lane i and potential vehicular relays in lane j . $\lambda_V^{(i,j)}$ and $\mu_V^{(i,j)}$ denote the arrival and departure rates of V2V link blockages, respectively. For this model, we denote the V2V sidelink blockage probability by $P_{V2V}^{(i,j)}$, which is the probability that the V2V sidelink between a designated CV in lane i and a relay CV in lane j is blocked, for $i, j = 1, \dots, N_L$. By using the steady-state solution of a two-state Markov chain, we have

$$P_{V2V}^{(i,j)} = \lambda_V^{(i,j)} / (\lambda_V^{(i,j)} + \mu_V^{(i,j)}). \quad (8)$$

As an example evolution of the Markov chain, consider a scenario where a reference CV in lane i has an LOS V2V link with another CV in lane j , which indicates that the system is in state L . For this example, let us assume without loss of generality that $i \geq j$. When this link gets blocked by a BV in lane j' , $j' = j, \dots, i$, the reference CV tries to find an alternate LOS path with another CV that resides in its LOS communication range. If it succeeds, then the system remains in state L . However, if no such path exists, the system transitions into state B . When an LOS V2V link is reestablished, the system transitions back into state L and so on. Note that this system only models the LOS state of V2V links, which may or may not serve as a relay, depending on whether the relay CV is in coverage by an RSU with an LOS V2I link. The rates of this model, which have a unit of $1/\text{s}$, will be used together with the V2I blockage probabilities in Section IV-B to characterize the entire vehicular relay network.

The transition rates of the V2V system in Figure 4 depends strictly on the modeling of specific vehicle movements, such as lane changing and vehicle passing. Therefore, we propose using either a simulation environment as in [10], or do a field measurement similar to the studies in [11], [14] with the vehicular scenario of interest, in order to obtain

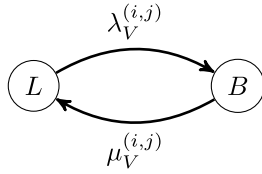


FIGURE 4. V2V link availability process for a reference CV in lane i and a destination CV in lane j for $i, j = 1, \dots, N_L$. L and B denote LOS and blocked states, respectively.

the transition rates of the V2V system. In this paper, similar to the methodology in [10], we run simulations for the desired combinations of i and j for a given set of parameters to obtain the transition rates $\lambda_V^{(i,j)}$ and $\mu_V^{(i,j)}$. For this purpose, we build and use a relatively simple simulation environment where vehicles are allowed to pass each other in the same lane, i.e., there is no lane switching. We also denote the fixed width of BV by w_B , which is chosen $w_B > 0$ in V2V link simulations, in order to model the blockages in the same lane and neighboring lanes. Analytically modeling the vehicular movements and obtaining the state transition rates of V2V LOS links is beyond the scope of this paper.

IV. COVERAGE ANALYSIS

In this section, we model the blockages of V2I and V2V links by using two separate continuous time Markov chain formulations, and discuss how we combine the steady-state solutions of these two Markov chains to obtain the blockage probability, average blockage duration, and the SINR distribution of the entire system. We start with the assumption that V2I and V2V links are blocked independently from each other, which enables the formulation of these two systems separately. We note here that in a real highway setting and in our simulation environment, V2I and V2V link blockages are correlated. For instance, a BV blocking a V2I link in lane j can also block the V2V links to relay CVs in lanes $j' = 1, \dots, j$, if the BV intersects the LOS path of V2V links. However, as we show in the numerical examples, simulations results, in which we relax all of our assumptions and simulate the actual highway environment, are in good agreement with the results obtained by the proposed analytical framework.

A. MARKOV CHAIN MODEL OF V2I LINKS

We denote the state space of the V2I Markov chain by \mathcal{S} . There are a total of $2^{(i-1)N_R}$ states in state space \mathcal{S} , and each state is represented by $(i-1)N_R$ binary bits, where i is the CV lane. The bits from $(n-1)(i-1)+1$ through $n(i-1)$ represent the blockage state of lane $j = 1, \dots, i-1$, respectively, for the LOS link connecting the CV to the n -th RSU, for $n = 1, \dots, N_R$. Specifically, if a BV in lane j for $j = 1, \dots, i-1$ is blocking the LOS link of n -th RSU, then $((n-1)(i-1)+j)$ -th bit of the state is set to 1, or to 0 otherwise. For example, state (011) is used to represent the case where $N_R = 1$, and BVs in lanes 1 and 2 are blocking the LOS link, whereas lane 3 is not blocking.

1) V2I MARKOV CHAIN STATE TRANSITIONS

In order to obtain the state transition rates in \mathcal{S} , we first define the speed of the projection of an RSU in lane j for a CV in lane i , denoted by $V_R^{(i,j)}$ for $i = 2, \dots, N_L$ and $j = 1, \dots, i-1$, as follows:

$$V_R^{(i,j)} = V_C \frac{j-1/2}{i-1/2}. \quad (9)$$

$V_R^{(i,j)}$ measures the relative speed of the projection of an RSU for each potentially blocking lane. For example, for a CV moving with a speed of V_C in lane $i = 3$, if we consider the LOS link connecting the CV with a given RSU, the projection of the RSU, which is the intersection point of the V2I link with the center of the blocking lanes $j = 1$ and $j = 2$, move with a speed of $0.2V_C$ and $0.6V_C$, respectively.

With $V_R^{(i,j)}$, we obtain the following two lemmas that characterize the transition rates for blocker arrivals and blockage duration.

Lemma 1: For a CV in lane i , the LOS coverage duration in lane j is exponentially distributed with rate $\lambda_B^{(i,j)} |V_B - V_R^{(i,j)}|$, for $i = 2, \dots, N_L, j = 1, \dots, i-1$, with $\lambda_B^{(i,j)}$ defined as in (4).

Proof: First, consider the case $V_B \geq V_R^{(i,j)}$. For a given RSU, the speed of the blockers relative to the projection of the RSU in lane j is $V_B - V_R^{(i,j)}$. Assume that the next blocker is at a distance of l . This results in a coverage duration of $l/(V_B - V_R^{(i,j)})$. Since l is distributed according to an exponential distribution with rate $\lambda_B^{(i,j)}$, the coverage duration is also exponentially distributed with mean $(\lambda_B^{(i,j)}(V_B - V_R^{(i,j)}))^{-1}$. A similar argument for the case $V_B < V_R^{(i,j)}$ also holds, which completes the proof. ■

Lemma 2: The duration of a blockage due to a BV in lane j is exponentially distributed with rate $\mu_B |V_B - V_R^{(i,j)}|$, for $i = 2, \dots, N_L, j = 1, \dots, i-1$, where $1/\mu_B$ is the average BV length.

Proof: We follow a similar argument as in the proof of Lemma 1. Given the BV length l , the RSU projection in lane j has to cover a distance of l with a relative speed of $|V_B - V_R^{(i,j)}|$ with respect to the BV. Since l follows an exponential distribution with rate μ_B , the LOS blockage duration is also exponentially distributed with mean $(\mu_B |V_B - V_R^{(i,j)}|)^{-1}$, which completes the proof. ■

For i given, we define $\lambda_j \triangleq \lambda_B^{(i,j)} |V_B - V_R^{(i,j)}|$ and $\mu_j \triangleq \mu_B |V_B - V_R^{(i,j)}|$. Let $s = (s_1, \dots, s_n, \dots, s_{N_R})$ denote the current state of the system, where s_n denotes the state of n -th RSU and has a length of $i-1$, for $n = 1, \dots, N_R$. With the transition rates defined in lemmas IV-A.1 and IV-A.1, we construct the Markov chain using the following state transitions.

- *Blockage arrivals on a lane:* For any state s_n for $n = 1, \dots, N_R$ whose j -th bit is 0 for $j = 1, \dots, i-1$, the transition rate to a lane blockage state s'_n is λ_j , where s_n and s'_n are the same except the j -th bit of s'_n is 1.

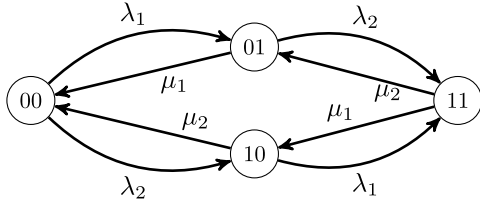


FIGURE 5. Markov chain model of V2I links for $N_R = 1$ and a CV in lane $i = 3$.

- **Blockage departure on a lane:** For any state s_n for $n = 1, \dots, N_R$ whose j -th bit is 1 for $j = 1, \dots, i - 1$, the transition rate to a coverage state s'_n is μ_j , where s_n and s'_n are the same except the j -th bit of s'_n is 0.

We illustrate a simple example of the Markov chain model of V2I blockages with state transitions in Figure 5, for $N_R = 1$, and $i = 3$. For this scenario, states denoted by (11), (01) and (10) correspond to the cases where at least one lane blocks the LOS link, hence, the CV is blocked. Thus, by using the steady-state probability of the blocked state (00) and the total transition rate out of it, we can obtain the blockage and coverage probabilities as well as the average blockage duration of the V2I links. We next generalize this idea for any number of RSUs and lanes.

2) BLOCKAGE PROBABILITY OF V2I LINKS

Let \mathcal{S}_B and \mathcal{S}_C denote the sets of states for which the CV is blocked and in coverage, respectively. We also denote the steady-state probability of state s by π_s , $\forall s \in \mathcal{S}$. For a given state space and its infinitesimal generator matrix, denoted by \mathbf{Q} , the steady-state probability distribution vector $\boldsymbol{\pi} = [\pi_1, \dots, \pi_{|\mathcal{S}|}]$ can be obtained by solving $\boldsymbol{\pi}\mathbf{Q} = \mathbf{0}_{1 \times |\mathcal{S}|}$, with the additional constraint $\sum_{s \in \mathcal{S}} \pi_s = 1$, where $|\mathcal{S}|$ denotes the cardinality of set \mathcal{S} . After obtaining $\boldsymbol{\pi}$, we compute the blockage probability of V2I links for a CV in lane i , denoted by $P_{V2I}^{(i)}$, as follows:

$$P_{V2I}^{(i)} = \sum_{s \in \mathcal{S}_B} \pi_s. \quad (10)$$

3) AVERAGE BLOCKAGE DURATION OF V2I LINKS

We denote the transition rate from state s to state s' by $r_{ss'}$. In order to compute the average blockage duration for a given Markov model of V2I links, we first compute the total normalized transition rate from unblocked states to blocked states, denoted by r_B , as follows:

$$r_B = \sum_{s \in \mathcal{S}_C} \sum_{s' \in \mathcal{S}_B} r_{ss'}. \quad (11)$$

Given state $s = \{s_1, s_2, \dots, s_{N_R}\}$, recall that state s_n for $n = 1, \dots, N_R$ is the binary number representing the blockage state of the n -th RSU. Let $|s_n|$ denote the number of ones in the binary number s_n , which is the number of blocking lanes for the n -th RSU. We define $N_s \triangleq \min\{|s_1|, \dots, |s_{N_R}|\}$ as the minimum number of blocking lanes that the CV has to pass across all N_R RSUs in order to regain coverage. For

instance, for the cases $s = \{(00), (01)\}$ and $s' = \{(01), (11)\}$, $N_s = \min\{0, 1\} = 0$ and $N_{s'} = \min\{1, 2\} = 1$, respectively.

By using Little's law [43], we obtain the following theorem to compute the average blockage duration of V2I links for a CV in lane i , which is denoted by $\bar{T}_{V2I}^{(i)}$.

Theorem 1: For a CV in lane i , for $i = 2, \dots, N_L$, the average blockage duration of V2I links is given by

$$\bar{T}_{V2I}^{(i)} = \frac{\mathbb{E}[N_s]}{r_B}, \quad (12)$$

where $\mathbb{E}[N_s]$ denotes the expected value of N_s over all $s \in \mathcal{S}_B$, computed as

$$\mathbb{E}[N_s] = \sum_{s \in \mathcal{S}_B} \pi_s N_s. \quad (13)$$

Proof: Little's law states that for any system with a given average job arrival rate and service time, their product gives the average number of jobs in the system. Let us consider the set of blocked states \mathcal{S}_B as the system with random arrivals and departures. The average arrival rate into the system r_B is given by (11). Moreover, the average number of blocking lanes for states $s \in \mathcal{S}_B$ is $\mathbb{E}[N_s]$ as given by (13). Hence, the average time spent in the system, or the expected blockage duration of V2I links, can be obtained directly by using Little's law as $\mathbb{E}[N_s]/r_B$. ■

Finally, we denote the average V2I coverage duration for a CV in lane i by $\bar{T}_C^{(i)}$. Note that the blockage probability can also be computed as $\bar{T}_{V2I}^{(i)}/(\bar{T}_C^{(i)} + \bar{T}_{V2I}^{(i)})$. Thus, $\bar{T}_C^{(i)}$ can be obtained as:

$$\bar{T}_C^{(i)} = \bar{T}_{V2I}^{(i)} \cdot \frac{1 - P_{V2I}^{(i)}}{P_{V2I}^{(i)}}. \quad (14)$$

B. MARKOV CHAIN MODEL OF VEHICULAR RELAYS

We denote the state space of the vehicular relays by \mathcal{S}' . A state in state space \mathcal{S}' is represented by N_L binary bits. j -th bit of a state is set to one or zero, indicating that the CV can or cannot be covered by a vehicular relay in lane j , respectively, for $j = 1, \dots, N_L$. Note that even if there is a V2V link between two CVs, the relay CV needs to be covered by an RSU in order to be used as a relay. Since each bit can take binary values, state space \mathcal{S}' consists of 2^{N_L} states.

1) VEHICULAR RELAY MARKOV CHAIN STATE TRANSITIONS

In order to define the state transitions of the Markov chain model of vehicular relays, we use the V2V blockage arrival and departure rates $\lambda_V^{(i,j)}$ and $\mu_V^{(i,j)}$, as defined in Section III-F. For a CV in lane i , we define λ_j' as the blockage arrival rate to the vehicular relays in lane j . We compute λ_j' by using the following lemma.

Lemma 3: For a CV in lane i , the blockage arrival rate to the vehicular relays in lane j , denoted by λ_j' , for $j = 1, \dots, N_L$, can be approximated as follows:

$$\lambda_j' = \lambda_V^{(i,j)} \left(1 - P_{V2I}^{(j)}\right) + 1/\bar{T}_C^{(j)}. \quad (15)$$

Proof: By definition, $\lambda_V^{(i,j)}$ is the blockage arrival rate to a V2V link between the CV in lane i and a destination CV in lane j . Since each CV in lane j is in coverage by at least one RSU with probability $1 - P_{V2I}^{(j)}$, and V2V and V2I links are blocked independently from each other, the blockage arrival rate to the vehicular relays is the blockage arrival rate of V2V links, thinned by the coverage probability $1 - P_{V2I}^{(j)}$. On the other hand, a relay in lane j is covered by V2I links for an average duration of $\bar{T}_C^{(j)}$. In other words, the blockage arrival rate to V2I links of a relay is $1/\bar{T}_C^{(j)}$. Since the arrivals of blockages to relay links and V2I links are assumed to be independent, the total blockage arrival rate is the sum of the corresponding individual blockage arrival rates, which completes the proof. ■

Similarly, for a CV in lane i , we define μ_j' as the blockage departure rate from the vehicular relays in lane j , which is given by the following lemma.

Lemma 4: For a CV in lane i , the blockage departure rate from the vehicular relays in lane j , denoted by μ_j' , for $j = 1, \dots, N_L$, can be approximated as follows:

$$\mu_j' = \mu_V^{(i,j)} \left(1 - P_{V2I}^{(j)}\right) P_{V2V}^{(i,j)} + \left(1 - P_{V2V}^{(i,j)}\right) P_{V2I}^{(j)} / \bar{T}_{V2I}^{(j)}. \quad (16)$$

Proof: We follow similar arguments as in the proof of Lemma 3. When a CV is connected through a relay, a blockage can depart either from the V2V sidelink if the relay is already connected to an RSU, or from a V2I link if the V2V sidelink is already connected. The first case occurs with probability $P_{V2V}^{(i,j)}$, and the corresponding blockage departure rate is $(1 - P_{V2I}^{(j)})\mu_V^{(i,j)}$. Similarly, V2I links are blocked with probability $P_{V2I}^{(j)}$ and the corresponding blockage departure rate is $(1 - P_{V2V}^{(i,j)})/\bar{T}_{V2I}^{(j)}$, since the blockage departure rate is equal to the reciprocal of the average blockage duration, $\bar{T}_{V2I}^{(j)}$. Due to the independent blockage assumption, the average blockage departure rate can be computed as the sum of the two rates, weighted by their corresponding probabilities. ■

With λ_j' and μ_j' defined, we have the following state transitions.

- *Blockage arrivals to vehicular relays:* For any state $s \in \mathcal{S}'$ whose j -th bit is 1 for $j = 1, \dots, N_L$, the transition rate to a vehicular relay blockage state s' is λ_j' , where s and s' are the same except the j -th bit of s' is 0.
- *Blockage departures from vehicular relays:* For any state $s \in \mathcal{S}'$ whose j -th bit is 0 for $j = 1, \dots, N_L$, the transition rate to a vehicular relay coverage state s' is μ_j' , where s and s' are the same except the j -th bit of s' is 1.

An example scenario with $i = N_L = 2$ is illustrated in Figure 6. Blockages to the vehicular relays in lane j arrive with a rate of λ_j' , whereas the departure rate of blockages for the vehicular relays in lane j is μ_j' , for $j = 1, 2$.

2) BLOCKAGE PROBABILITY OF VEHICULAR RELAYS

We denote the steady-state probability of state s by π_s' , $\forall s \in \mathcal{S}'$. Similarly, we denote the infinitesimal generator matrix

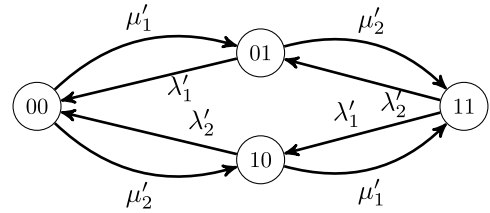


FIGURE 6. Markov chain model of vehicular relays for a CV in lane $i = N_L = 2$.

of \mathcal{S}' by \mathbf{Q}' . The steady-state probability distribution vector $\boldsymbol{\pi}' = [\pi_1', \dots, \pi_{|\mathcal{S}'|}']$ can be obtained by solving $\boldsymbol{\pi}'\mathbf{Q}' = \mathbf{0}_{1 \times |\mathcal{S}'|}$, with the additional constraint $\sum_{s \in \mathcal{S}'} \pi_s' = 1$. The only state with no vehicular relay in coverage is the state with all zero bits, which is the first state of the state space \mathcal{S}' . Therefore, the blockage probability of vehicular relays for a CV in lane i , denoted by $P_V^{(i)}$, is equal to the steady-state probability π_1' .

3) AVERAGE BLOCKAGE DURATION OF VEHICULAR RELAYS

The average blockage duration of vehicular relays is the average time spent in the first state, which is the state where all vehicular relays in lanes $j = 1, \dots, N_L$ are blocked. Note that the transition rate from this state to the state where there is a vehicular relay in lane j is μ_j' , which is the blockage departure rate from the vehicular relays in lane j , for $j = 1, \dots, N_L$. Therefore, we obtain the average blockage duration of vehicular relays for a CV in lane i , denoted by $\bar{T}_V^{(i)}$, as follows:

$$\bar{T}_V^{(i)} = \left(\sum_{j=1}^{N_L} \mu_j' \right)^{-1}, \quad (17)$$

since the average time spent in the blocked state is the reciprocal of the total transition rates out of this state.

C. OVERALL BLOCKAGE PROBABILITY

With the blockage probability of V2I links, $P_{V2I}^{(i)}$, and the blockage probability of vehicular relays, $P_V^{(i)}$, we can compute the overall blockage probability by using the following lemma.

Lemma 5: The overall blockage probability of a CV in lane i , denoted by P_B , is given by

$$P_B^{(i)} = P_{V2I}^{(i)} P_V^{(i)}. \quad (18)$$

Proof: The proof of the lemma follows directly from the independence of the blockages of V2I links and vehicular relays. ■

D. AVERAGE BLOCKAGE DURATION

Although the exact distributions of the blockage duration of V2I links and vehicular relays do not follow exponential distributions, we approximate each of these distributions by an exponential distribution. In particular, the blockage

duration of V2I links and vehicular relays are assumed to be exponentially distributed with rates $1/\bar{T}_{V2I}^{(i)}$ and $1/\bar{T}_V^{(i)}$, respectively. With this assumption, we use the following lemma to approximate the average blockage duration.

Lemma 6: The average blockage duration of a CV in lane i , denoted by $\bar{T}_B^{(i)}$, is approximated as

$$\bar{T}_B^{(i)} = \left(1/\bar{T}_{V2I}^{(i)} + 1/\bar{T}_V^{(i)}\right)^{-1}. \quad (19)$$

Proof: The blockage duration of V2I links and vehicular relays are independent and exponentially distributed with rates $1/\bar{T}_{V2I}^{(i)}$ and $1/\bar{T}_V^{(i)}$, respectively. Since the CV can be covered either by V2I links or vehicular relays, the blockage duration is the minimum of two exponential random variables with rates $1/\bar{T}_{V2I}^{(i)}$ and $1/\bar{T}_V^{(i)}$. Therefore, the blockage duration is also exponentially distributed with rate $1/\bar{T}_{V2I}^{(i)} + 1/\bar{T}_V^{(i)}$, which completes the proof. ■

E. SINR DISTRIBUTION ANALYSIS

The data rate that a CV experiences depends on whether it communicates with the network over a direct V2I link or through a relay, and the received SINR as given in (1). When the CV uses a direct V2I connection, it experiences a data rate of $W \log(1 + S)$, where S and W denotes the SINR of the V2I link and the channel bandwidth, respectively. On the other hand, if the CV uses a vehicular relay to reach the network, the experienced data rate depends on the SINR of both V2V and V2I links. We assume that each potential relay vehicle is equipped with at least two radio frequency (RF) chains; hence, during data exchange, it can simultaneously receive data from the designated CV and transmit the data to the connected RSU. Let S_V and S_I denote the SINR of V2V sidelink and V2I link, respectively. Then, the overall data rate is limited by the link with smaller SINR and given by $W \log(1 + \min(S_V, S_I))$. We denote $S_E \triangleq \min(S_V, S_I)$, which we will refer to as the *effective SINR* for the coverage through a vehicular relay.

For simplicity, we set the transmit power to 1 W, i.e., $P_T = 1$. We denote the random variable associated with the path loss by L . Given the path loss of a link $l = d^{-\alpha}$, the probability density function (pdf) of the received SINR, denoted by $f(s|l)$, is given by

$$f_{S|L}(s|l) = P\left(\frac{hl}{N_0} = s\right) = \mu e^{-\mu s N_0 / l}. \quad (20)$$

Removing the condition on the path loss, the SINR distribution can be obtained as

$$f_S(s) = \int f_{S|L}(s|l) f_L(l) dl = \int \mu e^{-\mu s N_0 / l} f_L(l) dl, \quad (21)$$

where $f_L(l)$ is the pdf of path loss.

The link length d and the resulting path loss l are random variables, whose values are determined by which relay and/or RSU the CV is connected to. We define d_{min} and d_{max} as the minimum and maximum link length of an LOS link, respectively, i.e., $d \in [d_{min}, d_{max}]$. Recall that the maximum

LOS link length is $d_{max} = R$ for both types of connections. On the other hand, the minimum link length can take different values for V2V and V2I links. As illustrated in Figure 2, d_{min} is equal to $(i-1/2)W_L$ for a V2I link. We set $d_{min} = W_L$ for a V2V link, which is the minimum distance between a CV and a vehicular relay in the neighboring lane.²

Assuming uniformly distributed link lengths between d_{min} and R , the pdf of the path loss can be obtained as follows:

$$f_L(l) = \begin{cases} \frac{l^{1/\alpha-1}}{\alpha(R-d_{min})}, & d_{min}^\alpha \leq l \leq R^\alpha, \\ 0, & \text{otherwise.} \end{cases} \quad (22)$$

For $\alpha = 2$, which is a typical value for LOS links, this implies that for uniformly distributed link lengths, the resulting path loss distribution $f_L(l)$ scales with $l^{-0.5}$. In a highway environment, the longer a V2V/V2I link is, the higher the probability that it is blocked, since the probability that a BV intersects the LOS link increases with the link length. Therefore, it is more probable to establish an LOS link with a relay/RSU that is within a shorter distance. Following this observation and (22), we model the pdf of the path loss as $f_L(l) = Al^{-1}$, where $A = (\alpha \ln(Rd_{min}))^{-1}$ is a constant satisfying

$$\int f_L(l) dl = \int_{d_{min}^\alpha}^{R^\alpha} Al^{-1} dl = 1. \quad (23)$$

Note that in a real vehicular environment, the distance distribution to relays, hence the path loss, can depend on the traffic density, which is parameterized by $E[d]$ in our analysis. Derivation of the SINR distribution for more general path-loss models is left as future work.

Proposition 2: For a link with length $d \in [d_{min}, R]$ and the path loss distribution $f_L(l) = Al^{-1}$, the corresponding SINR distribution can be written as

$$f_S(s) = A\mu \left(\Gamma\left(0, \frac{\mu s N_0}{R^\alpha}\right) - \Gamma\left(0, \frac{\mu s N_0}{d_{min}^\alpha}\right) \right), \quad (24)$$

where $\Gamma(\cdot)$ denotes the incomplete Gamma function.

Proof: Replacing $f_L(l)$ in (21) with Al^{-1} , we have

$$f_S(s) = \int_{d_{min}^\alpha}^{R^\alpha} \mu e^{-\mu s N_0 / l} Al^{-1} dl \quad (25)$$

$$= A\mu \int_{\mu s N_0 / d_{min}^\alpha}^{\mu s N_0 / R^\alpha} -\frac{e^{-u}}{u} du \quad (26)$$

$$= -A\mu \left(\int_{\mu s N_0 / d_{min}^\alpha}^{\infty} \frac{e^{-u}}{u} du - \int_{\mu s N_0 / R^\alpha}^{\infty} \frac{e^{-u}}{u} du \right) \quad (27)$$

$$= A\mu \left(\Gamma\left(0, \frac{\mu s N_0}{R^\alpha}\right) - \Gamma\left(0, \frac{\mu s N_0}{d_{min}^\alpha}\right) \right), \quad (28)$$

where we used $u = \mu s N_0 / l$ (26), and the definition of the Gamma function (28). ■

There can exist a vehicular relay in the CV lane which has a link length smaller than W_L . However, considering realistic inter-vehicle distances and vehicle lengths, we ignore such cases.

Corollary 1: The SINR distribution of the V2I links, denoted by $f_{S_I}(s)$, is given by

$$f_{S_I}(s) = A\mu \left(\Gamma \left(0, \frac{\mu s N_0}{R^\alpha} \right) - \Gamma \left(0, \frac{\mu s N_0}{((i-1/2)W_L)^\alpha} \right) \right). \quad (29)$$

Similarly, the SINR distribution of the V2V links, denoted by $f_{S_V}(s)$, can be written as

$$f_{S_V}(s) = A\mu \left(\Gamma \left(0, \frac{\mu s N_0}{R^\alpha} \right) - \Gamma \left(0, \frac{\mu s N_0}{W_L^\alpha} \right) \right). \quad (30)$$

Proof: The proof follows directly from Proposition 2 by replacing d_{min} with $(i-1/2)W_L$ and W_L for V2I and V2V links, respectively. ■

We define the following lemma to derive the cumulative distribution function (cdf) of the SINR, which will be used in the computation of the effective SINR distribution.

Lemma 8: The cdf of the SINR distribution given by (24) can be written as

$$F_S(s) = A\mu \left(\frac{R^\alpha}{\mu N_0} \left(1 - e^{-\frac{\mu s N_0}{R^\alpha}} \right) + s \Gamma \left(0, \frac{\mu s N_0}{R^\alpha} \right) - \frac{d_{min}^\alpha}{\mu N_0} \left(1 - e^{-\frac{\mu s N_0}{d_{min}^\alpha}} \right) - s \Gamma \left(0, \frac{\mu s N_0}{d_{min}^\alpha} \right) \right). \quad (31)$$

Proof: For tractability of the derivation, we first focus on the following integral:

$$\int_0^s \Gamma \left(0, \frac{\mu u N_0}{R^\alpha} \right) du = \int_0^s \int_{\frac{\mu u N_0}{R^\alpha}}^{\infty} e^{-x} x^{-1} dx du. \quad (32)$$

Changing the order of the integrals and the limits, (32) can be written as follows:

$$\begin{aligned} & \int_0^{\frac{\mu s N_0}{R^\alpha}} \int_0^{\frac{x R^\alpha}{\mu N_0}} e^{-x} x^{-1} du dx + \int_{\frac{\mu s N_0}{R^\alpha}}^{\infty} \int_0^s e^{-x} x^{-1} du dx \\ &= \int_0^{\frac{\mu s N_0}{R^\alpha}} \frac{e^{-x} R^\alpha}{\mu N_0} dx + \int_{\frac{\mu s N_0}{R^\alpha}}^{\infty} s e^{-x} x^{-1} dx \\ &= \frac{R^\alpha}{\mu N_0} \left(1 - e^{-\frac{\mu s N_0}{R^\alpha}} \right) + s \Gamma \left(0, \frac{\mu s N_0}{R^\alpha} \right). \end{aligned} \quad (33)$$

Given the pdf (24), we compute the cdf as

$$\begin{aligned} F_S(s) &= \int_0^s A\mu \left(\Gamma \left(0, \frac{\mu u N_0}{R^\alpha} \right) - \Gamma \left(0, \frac{\mu u N_0}{d_{min}^\alpha} \right) \right) du \\ &= A\mu \left(\int_0^s \Gamma \left(0, \frac{\mu u N_0}{R^\alpha} \right) du - \int_0^s \Gamma \left(0, \frac{\mu u N_0}{d_{min}^\alpha} \right) du \right). \end{aligned} \quad (34)$$

Plugging (33) into (34) completes the proof. ■

Similar to the corresponding pdfs, we obtain the cdfs of the SINR of V2I and V2V links by replacing d_{min} in (31) with $(i-1/2)W_L$ and W_L , respectively. In the following lemma, we derive the distribution of the effective SINR S_E of a connection through a vehicular relay.

Lemma 9: For a CV that is covered through a vehicular relay, the pdf of the effective SINR, denoted by $f_{S_E}(s)$, can be expressed as

$$f_{S_E}(s) = f_{S_I}(s)(1 - F_{S_V}(s)) + f_{S_V}(s)(1 - F_{S_I}(s)). \quad (35)$$

Proof: We can write the pdf $f_{S_E}(s)$ as follows:

$$f_{S_E}(s) = P(\min(S_I, S_V) = s) \quad (36)$$

$$= P(S_I = s, S_V \geq s) + P(S_V = s, S_I \geq s) \quad (37)$$

$$= P(S_I = s)P(S_V \geq s) + P(S_V = s)P(S_I \geq s) \quad (38)$$

$$= f_{S_I}(s)(1 - F_{S_V}(s)) + f_{S_V}(s)(1 - F_{S_I}(s)), \quad (39)$$

where we used the assumption of independence of V2V and V2I links, going from (37) to (38). ■

Theorem 2: Considering both direct V2I coverage and coverage through a relay, the SINR distribution of a CV, denoted by $f_{S_C}(s)$, is given by $f_{S_C}(s) =$

$$\begin{cases} \left(1 - P_{V2I}^{(i)} \right) f_{S_I}(s) + \left(1 - P_V^{(i)} \right) P_{V2I}^{(i)} f_{S_E}(s), & s > 0 \\ P_B^{(i)}, & s = 0. \end{cases} \quad (40)$$

Proof: The case $s = 0$ indicates that the CV is out of coverage, which occurs with probability $P_B^{(i)} = P_{V2I}^{(i)} P_V^{(i)}$. On the other hand, the CV can be covered with SINR $s > 0$ either over a direct V2I link, which happens with probability $1 - P_{V2I}^{(i)}$, or through a vehicular relay, with probability $P_{V2I}^{(i)}(1 - P_V^{(i)})$. Hence, by using the law of total probability, we can write the SINR distribution as follows:

$$f_{S_C}(s) = P(S_C = s) \quad (41)$$

$$= P(S_I = s) \left(1 - P_{V2I}^{(i)} \right) + P(S_E = s) \left(1 - P_V^{(i)} \right) P_{V2I}^{(i)} \quad (42)$$

$$= f_{S_I}(s) \left(1 - P_{V2I}^{(i)} \right) + f_{S_E}(s) \left(1 - P_V^{(i)} \right) P_{V2I}^{(i)}, \quad (43)$$

where we used the independence of V2I and V2I link states going from (41) to (42). ■

V. NUMERICAL RESULTS

We use MATLAB to implement a discrete-event simulator of the considered highway scenario. First, we randomly generate vehicles according to the highway and vehicle-related parameters; at each time step, the vehicles move with the specified speeds and then the LOS link state is checked. If a direct LOS V2I link is found between the CV and an RSU, the link state is recorded as *connected* and the next time step is executed. However, if all V2I links are blocked, all possible V2V sidelinks are calculated as candidate relay connections. If any of the candidate relays has a V2I connection to an RSU, then the link state is *connected*. However, if no path can be established through a relay to an RSU, then the link state is recorded as *blocked*. At each time step, blocked and connected intervals are checked and recorded for the calculation of blockage and coverage duration. For each data point illustrated in this section, we run the system for 10^9 time steps, or equivalently 10^9 ms, where we reinitialize the vehicle deployment every 10^5 ms. The MATLAB code for the discrete-event simulator is publicly available on GitHub [44].

The descriptions and values of the parameters that are fixed throughout the numerical examples are summarized in

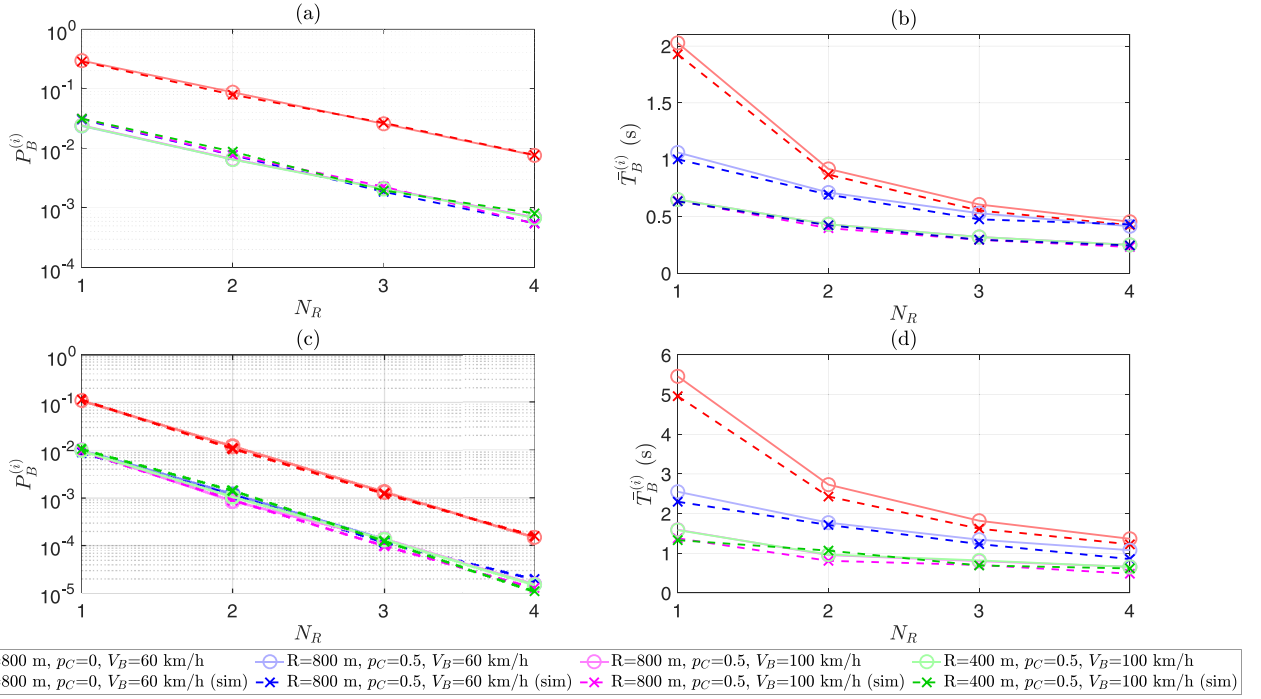


FIGURE 7. Blockage probability and average blockage duration as functions of the available number of RSUs N_R for (a), (b) $h_R = 2$ m and (c), (d) $h_R = 6$ m, $p_C \in \{0, 0.5\}$, $R \in \{400, 800\}$ m and $V_B \in \{60, 100\}$ km/h. Increasing the speed of BVs from 60 km/h to 100 km/h reduces the blockage duration, while the blockage probability remains constant. Having vehicular relays ($p_C = 0.5$) improves the performance in terms of both performance metrics, compared to the case with only V2I links ($p_C = 0$). Interestingly, increasing the LOS range while keeping N_R constant has marginal effect on the performance. Deployment of taller RSUs eliminates short term blockage events and drives up the average duration of the remaining blockages.

TABLE 1. Notation and values of parameters for examples I, II and III.

Parameter	Description	Value
V_B (km/h)	Speed of a BV	{60,100}
V_C (km/h)	Speed of a CV/SV	$1.2V_B$
h_C (m)	Height of a CV/SV	1.6
h_B (m)	Height of a BV	3
$1/\mu_C$ (m)	Average length of a CV/SV	5
$1/\mu_B$ (m)	Average length of a BV	13
h_R (m)	Height of an RSU	{2, 6}
N_R	Number of RSUs in coverage range	{1, 2, 3, 4}
p_B	BV probability	0.5
p_C	CV probability	[0, 0.5]
p_S	SV probability	$0.5 - p_C$
N_L	Number of lanes	4
i	CV lane	4
W_L (m)	Lane width	4
R (m)	mmWave LOS communication range	{200,400,800}
$E[d]$ (m)	Average inter-vehicle distance	{30,50,70}
μ	Rayleigh parameter	1
α	Path loss exponent	2

Table 1. For the given set of parameters and a CV in lane $i = N_L = 4$, we obtain the V2V link transition rates $\lambda_V^{(i,j)}$ and $\mu_V^{(i,j)}$ for $j = 1, 2, 3, 4$, and a BV width $w_B = 3$ m. We use these transition rates in the analytical solution.

In the first example, we validate the accuracy of our proposed analytical framework by comparing the results with those obtained by the discrete event simulator, for $E[d] = 50$ m, $h_R \in \{2, 6\}$, $p_C \in \{0, 0.5\}$, $V_B \in \{60, 100\}$ km/h, $R \in \{400, 800\}$ m and $N_R \in \{1, 2, 3, 4\}$. For all cases

the simulation results almost always overlap with the analytical solution in terms of the blockage probability, whereas there is a small gap for the average blockage duration. The first reason behind this phenomenon is that we assume blockages across V2I and V2V links occur independently from each other. However, in a real network, and also in our simulation environment, blockages can be correlated since a large vehicle can block multiple V2V and/or V2I links at the same time. Moreover, our assumption of exponentially distributed blockage duration for the relay and V2I links can lead to some inaccuracies in the results for the blockage duration. Nevertheless, the results are in good agreement with the simulations, which underscores the practicality and accuracy of the proposed analytical framework to analyze a vehicular relay network.

We observe from Figures 7(a) and 7(c) that the vehicle speeds do not affect the blockage probability, as expected, while faster vehicles result in shorter blockages on average as observed from Figures 7(b) and 7(d). The difference between $p_C = 0$ and $p_C = 0.5$ cases indicates that significant performance improvement can be achieved by utilizing V2V sidelinks and relays. On the other hand, interestingly, given that N_R is fixed, increasing the LOS range does not help reduce the blockage probability or the average blockage duration. This is due to the fact that the relays designated by a CV are usually at a relatively short distance from the CV as compared to the LOS range, since further away relays are blocked by BVs with higher probability. An alternative

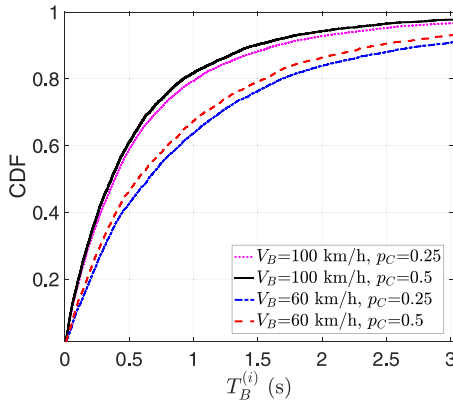


FIGURE 8. The cdf of the blockage duration for $V_B \in \{60, 100\}$ km/h and $p_C \in \{0.25, 0.5\}$. Increasing the CV probability shifts the cdf to the left for both speed values.

way to improve the performance might be to use multi-hop relaying scheme where relays are allowed to forward the traffic to another relay. However, for such systems, the operational complexities and overheads discussed in Section I such as the routing, scheduling, exponentially increasing traffic, etc., need to be further analyzed. Finally, we observe that deployment of taller RSUs eliminates short term blockage events. This reduces the blockage probability but drives up the average duration of the remaining blockages, which is also consistent with our findings in [25].

In our second example, we investigate how the blockage duration is distributed for different vehicle speeds and CV probabilities. For this purpose, we collect blockage data from the discrete-event simulator and plot the distributions of the recorded blockage durations in Figure 8, for $N_R = 1$, $h_R = 2$, $R = 400$ m and $E[d] = 50$ m. For fixed p_C , the blockage durations are significantly longer for $V_B = 60$ km/h compared to the case $V_B = 100$ km/h. The underlying reason is that the speed of a BV relative to the speed of the RSU projections as defined in (9) is larger for $V_B = 100$ km/h, hence blockages occur more frequently but are shorter. On the other hand, note that larger p_C potentially yields a higher number of candidate relays. For both vehicle speeds, having more candidate relays shifts the distribution of blockage duration to the left, indicating that relays help shorten the blockages.

Increasing traffic density causes more frequent blockages, but also provides a CV with more potential relays as link distances get smaller. Note that smaller inter-vehicle distance $E[d]$ is an indicator of higher traffic density and vice versa. In the third example, we vary $E[d]$ to examine the effects of traffic density on the performance. For $E[d] = 30, 50$ and 70 m, we vary p_C from 0 (no CVs) to 0.5 (all non-blocking vehicles are CVs) and demonstrate the blockage probability, average blockage duration and the cdf of the normalized SINR in Figures 9(a), 9(b) and 9(c), respectively. For other system parameters, we set $h_R = 2$ m, $N_R = 1$, $R = 200$ m and $V_B = 100$ km/h. We observe that as $E[d]$ decreases, a higher traffic density results in higher blockage

probability and lower SINR, but interestingly, lower average blockage duration for $p_C > 0.1$. This is because for p_C large enough, having closer relays with the increased traffic density can potentially provide more frequent but intermittent connections, which helps shorten the blockage duration. Although these intermittent relay connections reduce the average blockage duration, frequent blockages due to the high traffic density can also introduce significant packet retransmission delays. For some use cases, such as several advance driving scenarios and sensory information share, data from the interrupted transmissions can be discarded and *fresh* information can be transmitted once the connection is reestablished. However, for most of the V2X use cases, including autonomous driving/maneuvering and vehicle platooning, the radio access network needs to provide high reliability and manage link interruptions and the resulting retransmissions without requiring application-layer message retransmissions [45]. Retransmission of the packets buffered during blockages needs to be considered while designing the system as it can cause significant overhead and delay, depending on the use case and the type of data exchanged with the network. Higher layer mechanisms can be utilized to manage retransmissions, employing efficient resource allocation and scheduling techniques [46]. Finally, the change in the SINR distribution which is derived in (40) and illustrated in Figure 9(c) is due to the difference between the SINR distributions of V2I and relay links, and the changing blockage probability of V2I and relay links as traffic density varies.

VI. CONCLUSION

In this paper, we investigate the limitations of mmWave communication for vehicular networks, which is a promising technology to enable future vehicular use cases with the tremendous capacity it offers. We consider mmWave communications between CVs and RSUs, either over direct V2I links or through vehicular relays, in terms of blockage probability, average blockage duration, SINR distribution and distribution of blockage duration. To analyze the system, we establish Markov chain formulations of blockages that V2I links and vehicular relays experience, and by using their steady-state solutions, we obtain analytical expressions for the performance metrics of interest. We first validate that the results obtained by solving the proposed analytical model are in good agreement with those obtained by simulations for a wide set of parameters. We then examine the impact of different system parameters on the performance. Keeping the number of RSUs in the LOS communication range constant, we show that increasing the LOS communication range of a CV does not improve its coverage performance, since further away relays are blocked with a high probability. We demonstrate that V2V sidelinks and relays improve the system performance for different vehicle speeds. More interestingly, for high traffic densities, relays can reduce the average blockage duration by providing intermittent but frequent connection opportunities to the CV.

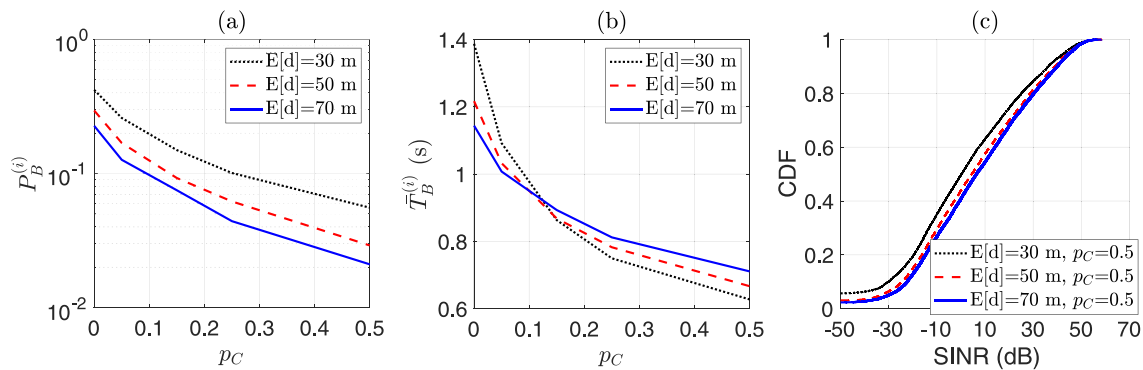


FIGURE 9. (a) Blockage probability and (b) average blockage duration as functions of CV probability p_C , for $E[d] \in \{30, 50, 70\}$ m, and (c) cdf of SINR, for $p_C = 0.5$ and $E[d] \in \{30, 50, 70\}$ m. Although smaller $E[d]$ indicates a higher traffic density and results in higher blockage probability and lower SINR, average blockage duration benefits from having more potential relays as the traffic density increases for $p_C > 0.1$. Simulation results for 9(a) and 9(b) are not displayed for clarity; they almost overlap the analytical results.

In future work, we will analyze a similar vehicular relay network with NLOS paths for V2V and V2I links. Also, in this paper, we assume extremely directional beams with very small beamwidths. Another interesting research direction to examine is to optimize the beamwidth in order to minimize blockages due to highly directional beams, while maintaining the coverage performance with the increased signal attenuation as the beamwidth increases.

REFERENCES

- [1] D. Amendola *et al.*, "Deliverable D2.1 5G CARMEN use cases and requirements," 5GCARMEN, Rep. D2.1, May 2019. Accessed: Jan. 31, 2021. [Online]. Available: https://5gcarmen.eu/wp-content/uploads/2020/03/5G_CARMEN_D2.1_FINAL.pdf
- [2] A. Osseiran *et al.*, "Scenarios for 5G mobile and wireless communications: The vision of the METIS project," *IEEE Commun. Mag.*, vol. 52, no. 5, pp. 26–35, May 2014.
- [3] I. Shayeia, M. Ergen, M. H. Azmi, S. A. Çolak, R. Nordin, and Y. I. Daradkeh, "Key challenges, drivers and solutions for mobility management in 5G networks: A survey," *IEEE Access*, vol. 8, pp. 172534–172552, 2020.
- [4] Y. Wang, K. Venugopal, A. F. Molisch, and R. W. Heath, "Blockage and coverage analysis with MmWave cross street BSs near urban intersections," in *Proc. IEEE ICC*, May 2017, pp. 1–6.
- [5] A. Tassi, M. Egan, R. J. Piechocki, and A. Nix, "Modeling and design of millimeter-wave networks for highway vehicular communication," *IEEE Trans. Veh. Technol.*, vol. 66, no. 12, pp. 10676–10691, Dec. 2017.
- [6] M. Giordani, M. Rebato, A. Zanella, and M. Zorzi, "Coverage and connectivity analysis of millimeter wave vehicular networks," *Ad Hoc Netw.*, vol. 80, pp. 158–171, Nov. 2018.
- [7] F. N. Alsaleem, J. S. Thompson, and D. I. Laurenson, "Adaptive sum of Markov chains for modelling 3D blockage in mmWave V2I communications," *IEEE Trans. Veh. Technol.*, vol. 69, no. 9, pp. 9431–9444, Sep. 2020.
- [8] C. Tunc, M. F. Özkoc, and S. Panwar, "Millimeter wave coverage and blockage duration analysis for vehicular communications," in *Proc. IEEE 90th Veh. Technol. Conf. (VTC-Fall)*, 2019, pp. 1–6.
- [9] M. K. Abdel-Aziz, C.-F. Liu, S. Samarakoon, M. Bennis, and W. Saad, "Ultra-reliable low-latency vehicular networks: Taming the age of information tail," in *Proc. IEEE GLOBECOM*, Dec. 2018, pp. 1–7.
- [10] M. Boban, X. Gong, and W. Xu, "Modeling the evolution of line-of-sight blockage for V2V channels," in *Proc. IEEE 84th VTC-Fall*, 2016, pp. 1–7.
- [11] A. Yamamoto, K. Ogawa, T. Horimatsu, A. Kato, and M. Fujise, "Path-loss prediction models for intervehicle communication at 60 GHz," *IEEE Trans. Veh. Technol.*, vol. 57, no. 1, pp. 65–78, Jan. 2008.
- [12] S. Chen, K. Vu, S. Zhou, Z. Niu, M. Bennis, and M. Latva-Aho, "A deep reinforcement learning framework to combat dynamic blockage in mmWave V2X networks," in *Proc. 2nd 6G SUMMIT*, 2020, pp. 1–5.
- [13] S. Rangan, T. S. Rappaport, and E. Erkip, "Millimeter-wave cellular wireless networks: Potentials and challenges," *Proc. IEEE*, vol. 102, no. 3, pp. 366–385, Mar. 2014.
- [14] M. Boban *et al.*, "Multi-band vehicle-to-vehicle channel characterization in the presence of vehicle blockage," *IEEE Access*, vol. 7, pp. 9724–9735, 2019.
- [15] R. Ford, M. Zhang, M. Mezzavilla, S. Dutta, S. Rangan, and M. Zorzi, "Achieving ultra-low latency in 5G millimeter wave cellular networks," *IEEE Commun. Mag.*, vol. 55, no. 3, pp. 196–203, Mar. 2017.
- [16] M. R. Akdeniz *et al.*, "Millimeter wave channel modeling and cellular capacity evaluation," *IEEE J. Sel. Areas Commun.*, vol. 32, no. 6, pp. 1164–1179, Jun. 2014.
- [17] G. R. MacCartney, T. S. Rappaport, and S. Rangan, "Rapid fading due to human blockage in pedestrian crowds at 5G millimeter-wave frequencies," in *Proc. IEEE GLOBECOM*, Dec. 2017, pp. 1–7.
- [18] I. K. Jain, R. Kumar, and S. S. Panwar, "The impact of mobile blockers on millimeter wave cellular systems," *IEEE J. Sel. Areas Commun.*, vol. 37, no. 4, pp. 854–868, Apr. 2019.
- [19] S. Lien *et al.*, "3GPP NR sidelink transmissions toward 5G V2X," *IEEE Access*, vol. 8, pp. 35368–35382, 2020.
- [20] "Study on vehicle-mounted relays, stage 1, version release 18," 3GPP, Sophia Antipolis, France, Rep. TR 22.839, 2021.
- [21] V. Sharma, I. You, and N. Guizani, "Security of 5G-V2X: Technologies, standardization, and research directions," *IEEE Netw.*, vol. 34, no. 5, pp. 306–314, Sep./Oct. 2020.
- [22] P. Liu, Z. Tao, S. Narayanan, T. Korakis, and S. S. Panwar, "CoopMAC: A cooperative MAC for wireless LANs," *IEEE J. Sel. Areas Commun.*, vol. 25, no. 2, pp. 340–354, Feb. 2007.
- [23] S. C. Ng, W. Zhang, Y. Zhang, Y. Yang, and G. Mao, "Analysis of access and connectivity probabilities in vehicular relay networks," *IEEE J. Sel. Areas Commun.*, vol. 29, no. 1, pp. 140–150, Jan. 2011.
- [24] V. Ramaiyan, E. Altman, and A. Kumar, "Delay optimal scheduling in a two-hop vehicular relay network," *Mobile Netw. Appl.*, vol. 15, no. 1, pp. 97–111, 2010.
- [25] C. Tunc, M. F. Özkoc, F. Fund, and S. S. Panwar, "The blind side: Latency challenges in millimeter wave networks for connected vehicle applications," *IEEE Trans. Veh. Technol.*, vol. 70, no. 1, pp. 529–542, Jan. 2021, doi: [10.1109/TVT.2020.3046501](https://doi.org/10.1109/TVT.2020.3046501).
- [26] Y. Wang, K. Venugopal, A. F. Molisch, and R. W. Heath, "MmWave vehicle-to-infrastructure communication: Analysis of urban micro-cellular networks," *IEEE Trans. Veh. Technol.*, vol. 67, no. 8, pp. 7086–7100, Aug. 2018.
- [27] K. Satyanarayana, M. El-Hajjar, A. A. M. Mourad, and L. Hanzo, "Deep learning aided fingerprint-based beam alignment for mmWave vehicular communication," *IEEE Trans. Veh. Technol.*, vol. 68, no. 11, pp. 10858–10871, Nov. 2019.
- [28] M. Giordani, A. Zanella, and M. Zorzi, "LTE and millimeter waves for V2I communications: An end-to-end performance comparison," in *Proc. IEEE 89th VTC-Spring*, 2019, pp. 1–7.

- [29] L. Kong, M. K. Khan, F. Wu, G. Chen, and P. Zeng, "Millimeter-wave wireless communications for IoT-cloud supported autonomous vehicles: Overview, design, and challenges," *IEEE Commun. Mag.*, vol. 55, no. 1, pp. 62–68, Jan. 2017.
- [30] M. Giordani, A. Zanella, T. Higuchi, O. Altintas, and M. Zorzi, "Performance study of LTE and mmWave in vehicle-to-network communications," in *Proc. IEEE 17th Med-Hoc-Net*, 2018, pp. 1–7.
- [31] Y. Kang, H. Seo, and W. Choi, "When to realign the receive beam in high mobility V2X communications?" *IEEE Trans. Veh. Technol.*, vol. 69, no. 11, pp. 13180–13195, Nov. 2020.
- [32] M. G. Nilsson, C. Gustafson, T. Abbas, and F. Tufvesson, "A measurement-based multilink shadowing model for V2V network simulations of highway scenarios," *IEEE Trans. Veh. Technol.*, vol. 66, no. 10, pp. 8632–8643, Oct. 2017.
- [33] Z. Li, L. Xiang, X. Ge, G. Mao, and H.-C. Chao, "Latency and reliability of mmWave multi-hop V2V communications under relay selections," *IEEE Trans. Veh. Technol.*, vol. 69, no. 9, pp. 9807–9821, Sep. 2020.
- [34] B. R. Elbal, S. Schwarz, and M. Rupp, "Relay selection and coverage analysis of relay assisted V2I links in microcellular urban networks," in *Proc. IEEE Wireless Commun. Netw. Conf. (WCNC)*, 2020, pp. 1–7.
- [35] A. Taya, T. Nishio, M. Morikura, and K. Yamamoto, "Coverage expansion through dynamic relay vehicle deployment in mmWave V2I communications," in *Proc. IEEE 87th Veh. Technol. Conf. (VTC Spring)*, 2018, pp. 1–5.
- [36] Y. Feng, D. He, Y. Guan, Y. Huang, Y. Xu, and Z. Chen, "Beamwidth optimization for millimeter-wave V2V communication between neighbor vehicles in highway scenarios," *IEEE Access*, vol. 9, pp. 4335–4350, 2021.
- [37] X. Ge, "Ultra-reliable low-latency communications in autonomous vehicular networks," *IEEE Trans. Veh. Technol.*, vol. 68, no. 5, pp. 5005–5016, May 2019.
- [38] M. Fallgren *et al.*, "Fifth-generation technologies for the connected car: Capable systems for Vehicle-to-Anything communications," *IEEE Veh. Technol. Mag.*, vol. 13, no. 3, pp. 28–38, Sep. 2018.
- [39] C.-F. Liu and M. Bennis, "Ultra-reliable and low-latency vehicular transmission: An extreme value theory approach," *IEEE Commun. Lett.*, vol. 22, no. 6, pp. 1292–1295, Jun. 2018.
- [40] "Study on evaluation methodology of new Vehicle-to- Everything (V2X) use cases for LTE and NR, version 15.3.0, release 15," 3GPP, Sophia Antipolis, France, Rep. TR 37.885, 2019.
- [41] T. Shimizu, V. Va, G. Bansal, and R. W. Heath, "Millimeter wave V2X communications: Use cases and design considerations of beam management," in *Proc. AMPC*, 2018, pp. 183–185.
- [42] J. Wang, W. Zhang, X. Bao, T. Song, and C. Pan, "Outage analysis for intelligent reflecting surface assisted vehicular communication networks," 2020. [Online]. Available: arXiv:2004.08063v2.
- [43] J. D. C. Little, "A proof for the queuing formula: $L = \lambda W$," *Oper. Res.*, vol. 9, no. 3, pp. 383–387, 1961.
- [44] C. Tunc. *Millimeter Wave (mmWave)-Enabled Vehicular Relay Network Simulation*. Accessed: Jun. 3, 2021. [Online]. Available: <https://github.com/caglarTunc/vehicularRelay>
- [45] "Study on enhancement of 3GPP support for 5G V2X services, v16.2.0, release 16," 3GPP, Sophia Antipolis, France, Rep. TR 22.886, 2018.
- [46] S. E. Elayoubi, P. Brown, M. Deghel, and A. Galindo-Serrano, "Radio resource allocation and retransmission schemes for URLLC over 5G networks," *IEEE J. Sel. Areas Commun.*, vol. 37, no. 4, pp. 896–904, Apr. 2019.



CAGLAR TUNC (Graduate Student Member, IEEE) received the B.S. and M.S. degrees from the Department of Electrical and Electronics Engineering, Bilkent University, Ankara, Turkey, in 2013 and 2016, respectively. He is currently pursuing the Ph.D. degree with the Department of Electrical and Computer Engineering, NYU Tandon School of Engineering. His research interests are in wireless communications, signal processing, and stochastic modeling of networked systems.



SHIVENDRA S. PANWAR (Fellow, IEEE) received the Ph.D. degree in electrical and computer engineering from the University of Massachusetts, Amherst, MA, USA, in 1986. He is currently a Professor with the Electrical and Computer Engineering Department, NYU Tandon School of Engineering. He is also the Director of the New York State Center for Advanced Technology in Telecommunications, the Co-Founder of the New York City Media Lab, and a Member of NYU Wireless. His research interests include the performance analysis and design of networks. He has coauthored a textbook titled *TCP/IP Essentials: A Lab Based Approach* (Cambridge University Press). His current research focuses on cross-layer research issues in wireless networks, and multimedia transport over networks. He was a winner of the IEEE Communication Society's Leonard Abraham Prize for 2004, the ICC Best Paper Award in 2016, and the Sony Research Award. He was also co-awarded the Best Paper in 2011 Multimedia Communications Award. He has served as the Secretary for the Technical Affairs Council of the IEEE Communications Society.